

Study of Langmuir monolayers of ruthenium complexes and their aggregation by electrogenerated chemiluminescence

Cary J. Miller, Paul. McCord, and Allen J. Bard

Langmuir, 1991, 7 (11), 2781-2787 • DOI: 10.1021/la00059a061

Downloaded from <http://pubs.acs.org> on January 23, 2009

More About This Article

The permalink <http://dx.doi.org/10.1021/la00059a061> provides access to:

- Links to articles and content related to this article
- Copyright permission to reproduce figures and/or text from this article



ACS Publications
High quality. High impact.

Study of Langmuir Monolayers of Ruthenium Complexes and Their Aggregation by Electrogenerated Chemiluminescence

Cary J. Miller,[†] Paul McCord, and Allen J. Bard*

Department of Chemistry and Biochemistry, The University of Texas at Austin, Austin, Texas 78712

Received May 28, 1991

Monolayer films of $\text{Ru}(\text{bpy})_2(\text{bpy}-\text{C}_{19})^{2+}$ and $\text{Ru}(\text{dp}-\text{bpy})_3^{2+}$, on a Langmuir trough contacted by the horizontal touch (HT) method with an indium-tin oxide (ITO) coated glass or a highly oriented pyrolytic graphite (HOPG) electrode, are characterized by imaging of their electrogenerated chemiluminescent (ECL) emission. ECL photographs of the Ru complexes suggest that aggregation of these amphiphiles occurs prior to their compression. In addition to the ECL measurements, pressure/area isotherms and cyclic voltammetry were used to study the behavior of these Ru complexes at the air/water interface.

Introduction

We consider here monolayers of ruthenium complexes at the air/aqueous subphase interface and, when contacted by an electrode surface, their characterization by electrogenerated chemiluminescence (ECL). Two different Ru complexes are considered; their structures are shown in Figure 1. The first, $\text{Ru}(\text{bpy})_2(\text{bpy}-\text{C}_{19})^{2+}$, studied previously,¹ with a long hydrocarbon tail, is typical of molecules that form Langmuir monolayers. The second, $\text{Ru}(\text{dp}-\text{bpy})_3^{2+}$,² while fairly insoluble in the aqueous subphase, is a nonconventional monolayer molecule. With the increasing interest in Langmuir monolayers and multilayer assemblies transferred onto solid supports by the Langmuir-Blodgett method, the development of characterization techniques for these thin organic films has become more and more important.³ Techniques are needed to study monolayer structure, degree of ordering, uniformity, and stability. For example, imaging of monolayer and submonolayer coverages of luminophores by fluorescence microscopy has been used in the characterization of monolayer films.⁴ ECL imaging, which involves the electrogeneration of species which react to form excited states, can address several of these issues, particularly the uniformity of ECL-active molecules transferred onto electrode surfaces.⁵ Photographs of the ECL emission give a direct measure of the deposition pattern of an ECL-active probe on the electrode surface. In addition to the spatial distribution of the probe on the electrode, some information related to the local environment of the luminescent probe can be inferred from the intensity of the ECL emission, which is strongly dependent on the quenching of the luminescent molecule by the electrode and by neighboring molecular quenchers. We previously described^{6,7} "on-trough" electrochemical studies of films at the air/aqueous subphase interface in which the film was brought into contact with an electrode using the

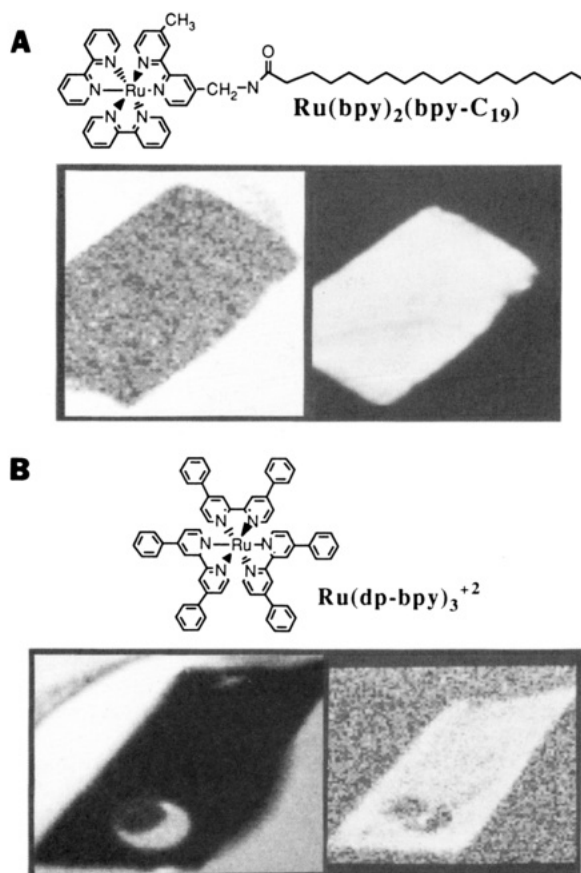


Figure 1. ECL photographs of monolayers of (A) $\text{Ru}(\text{bpy})_2(\text{bpy}-\text{C}_{19})^{2+}$ and (B) $\text{Ru}(\text{dp}-\text{bpy})_3^{2+}$ transferred to HOPG electrodes at surface coverages of 110 and 125 $\text{\AA}^2/\text{molecule}$, respectively. For these ECL photographs (right), the exposure time was 30 s. For comparison, photographs of the electrodes under external illumination taken just prior to the ECL measurements (left) are also shown. HOPG electrode size: 0.5 cm by 0.5 cm.

"horizontal touch" (HT) method.⁸ We now extend this approach to on-trough ECL photography of Langmuir monolayers of luminescent Ru complexes. The technique is also shown to be useful in the study of the aggregation of amphiphiles at the air/subphase interface at low surface coverages.

Much recent attention has been directed toward the formation and structure of highly conjugated, rigid am-

* To whom correspondence should be addressed.

[†] Present address: Department of Chemistry and Biochemistry, University of Maryland, College Park, MD 20742.

(1) Zhang, X.; Bard, A. J. *J. Phys. Chem.* **1988**, *92*, 5566.

(2) McCord, P.; Bard, A. J. *J. Electroanal. Chem.*, in press.

(3) Swalen, J. D.; Allara, D. L.; Andrade, J. D.; Chandross, E. A.; Garoff, S.; Israelachvili, J. T.; MacCarthy, J.; Murray, R.; Pease, R. F.; Rabolt, J. F.; Wynne, K. J.; Yu, H. *Langmuir* **1987**, *3*, 932.

(4) Seul, M.; Subramaniam, S.; McConnell, H. M. *J. Phys. Chem.* **1985**, *89*, 3592.

(5) Obeng, Y. S.; Bard, A. J. *Langmuir* **1991**, *7*, 195.

(6) Zhang, X.; Bard, A. J. *J. Am. Chem. Soc.* **1989**, *111*, 8098.

(7) Miller, C. J.; Bard, A. J. *Anal. Chem.* **1991**, *63*, 1707.

(8) Langmuir, I.; Schaefer, V. J. *J. Am. Chem. Soc.* **1939**, *60*, 1351.

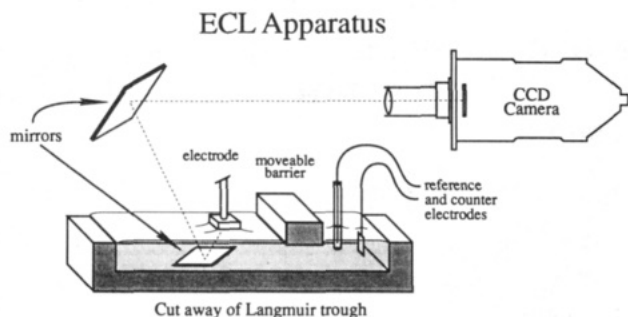


Figure 2. Schematic diagram of the on-trough ECL photography apparatus. The figure shows a cutaway drawing of a Teflon Langmuir trough filled with an aqueous subphase.

phiphiles for possible use in the fabrication of nonlinear optical films and molecular electronic devices.³ These amphiphiles generally form very "stiff" monolayers which tend to form two-dimensional crystallites or aggregates under low surface pressure conditions.⁹ The transfer of these films onto solid supports via the traditional Langmuir-Blodgett method can result in serious film defects. Characterization of the state of the monolayer film on the air/subphase interface is therefore of importance for the development of the optical and electrical uses of these films. Of particular interest is the relationship of the structure of the amphiphile to its viscoelastic properties in monolayer films on the Langmuir trough. In this work the level of aggregation of ECL-active ruthenium(II) complexes at the air/subphase interface at low surface pressures (0–0.1 mN/m) and the uniformity of monolayer films transferred to electrodes using the HT^{6,7} method are probed by ECL photography.

Experimental Section

Materials. The synthesis of Ru(bpy)₂(bpy-C₁₉)(ClO₄)₂ has been described previously.¹ Tris(4,7-diphenyl-1,10-phenanthroline)ruthenium(II) perchlorate, Ru(dpp)₃(ClO₄)₂, and tris(4,4'-diphenyl-2,2'-bipyridyl)ruthenium(II) perchlorate, Ru(dp-bpy)₃(ClO₄)₂, were synthesized using the procedure of Anderson et al.¹⁰ Tris(4,7-diphenyl-1,10-phenanthroline)iron(II) perchlorate, Fe(dpp)₃(ClO₄)₂, and tris(4,7-diphenyl-1,10-phenanthroline)cobalt(II) perchlorate, Co(dpp)₃(ClO₄)₂, were synthesized using a literature procedure.¹¹ All other chemicals were reagent grade and used as received. Aqueous solutions were prepared from water purified via an ion exchange purification train (Milli Q system, Millipore Inc.).

Indium-tin oxide (ITO) electrodes were cut from ITO-coated glass plates (Delta Technologies, Stillwater, MN). Highly ordered pyrolytic graphite (HOPG) electrodes were made from samples generously supplied by Dr. Arthur Moore (Union Carbide). Squares (0.3 cm²) of HOPG, ca. 0.05 mm thick, were mounted on the end of a 1-mm-diameter Cu wire using Ag epoxy cement (H20S from Epo-tek, Billerica, MA). The Cu wire was insulated with vacuum epoxy cement. Before all experiments, the electrodes were rinsed with EtOH and deionized H₂O and dried with a stream of purified Ar.

Apparatus. Figure 2 is a schematic drawing of the apparatus used for on-trough electrochemical studies and ECL photography of transferred monolayer films. A Langmuir trough was constructed of Teflon with a Teflon bar which allowed for the manual contraction and expansion of the air/subphase interface. As in previous on-trough electrochemistry,^{6,7} a Pt counter electrode and a Ag/AgCl/saturated KCl reference electrode were immersed in the subphase solution. For the ECL experiments, the trough was filled with 0.1 M NaClO₄ and 0.1 M Na₂C₂O₄ and the surface cleaned by repeated sweeping of the surface with the Teflon barrier while some of the subphase solution was aspirated from the surface of the trough. After the monolayer was deposited

onto the subphase surface, HOPG or ITO electrodes oriented with their surfaces parallel to the air/subphase interface were brought into contact with the monolayer-coated surface using a Lauda film balance lifter at a speed of 10 mm/s (HT transfer method). The electrodes were subsequently stepped to a potential of 1.2 V vs Ag/AgCl, oxidizing the surface-bound Ru complex which, in the presence of oxalate anions, initiated the ECL emission. The light emitted from the monolayer film was directed, by means of two mirrors positioned as indicated in Figure 2, toward a CCD camera (model CH210, Photometrics Ltd., Tucson, AZ) cooled to -90 °C.

Surface pressure/area isotherms were obtained using a Lauda preparative film balance, model P (Brinkman Instruments Co., Westbury, NY). Electrochemical experiments were performed using either a potentiostat connected to a function generator (model 173 and model 175, respectively, Princeton Applied Research, Princeton, NJ) or a BAS 100A electrochemical analyzer (Bioanalytical Systems Inc., West Lafayette, IN).

Results and Discussion

Principles of ECL Imaging. Imaging of monolayers by ECL compared very favorably with fluorescence photography. In a typical fluorescence apparatus, an intense monochromatic light source, typically a laser, is used to excite a fluorescent probe molecule within a monolayer film either at the air/subphase interface or on a solid support.⁴ The fluorescence emission from the monolayer is separated from the excitation wavelength and photographed. In an ECL experiment, the probe molecule is excited chemically through a series of redox reactions. The probe molecules chosen for study here are those based on the well-studied Ru(bpy)₃²⁺ system.^{12,13} A convenient excitation scheme for these ruthenium(II) complexes involves the oxidation of the complex in the presence of oxalate ion in aqueous solution.^{5,6,12} The Ru(III) centers in the monolayer oxidize the oxalate which decomposes to form CO₂ and CO₂⁻ radical anion. The CO₂⁻ reacts directly with the Ru(III) species, or reduces the Ru(II) complex to Ru(I) which undergoes a redox reaction with the Ru(III) species, producing an electronically excited Ru(II) center, which emits light.¹² Because the excitation of the Ru(II) centers is achieved chemically, there is no background emission or scattered light; this allows very sensitive detection of the emitted radiation. This low background characteristic can be exploited to develop extremely sensitive measurements of ECL-active molecules in solution.^{14,15} Because no laser excitation source or special filters are required for this technique, the optical system required for ECL photography is simplified over that used in fluorescence measurements.

To initiate the ECL, the Ru complexes must be oxidized to the Ru(III) oxidation state. This is achieved electrochemically by first depositing the monolayer onto the electrode using a horizontal touching (HT) transfer in which the electrode, oriented parallel to the air/subphase interface, is brought into contact with the monolayer-coated subphase. After the electrode (fabricated out of HOPG- or ITO-coated glass) makes contact with the subphase, it is stepped positive of the potential for oxidation of the Ru complex using a potentiostat connected with a reference and counter electrode placed in the trough, as shown in Figure 2.

Figure 1 shows ECL photographs of monolayers of Ru(dp-bpy)₃²⁺ and Ru(bpy)₂(bpy-C₁₉)²⁺ transferred onto HOPG electrodes near their limiting coverages (ca. 100

(12) Chang, M.-M.; Saji, T.; Bard, A. J. *J. Am. Chem. Soc.* **1977**, *99*, 5399.

(13) Tokel-Takvoryan, N. E.; Hemingway, R. E.; Bard, A. J. *J. Am. Chem. Soc.* **1973**, *95*, 6582.

(14) Ege, D.; Becker, W. G.; Bard, A. J. *Anal. Chem.* **1984**, *56*, 2413.

(15) Leland, J. K. Private communication.

(9) Lando, J. B.; Mann, J. A. *Langmuir* **1990**, *6*, 293.

(10) Anderson, S.; Seddon, K. R. *J. Chem. Res., Synop.* **1979**, 74.

(11) Burstall, F. H.; Nyholm, R. S. *J. Chem. Soc.* **1952**, 3570.

and $105 \text{ \AA}^2/\text{molecule}$, respectively). Also shown in Figure 1 are photographs of the electrodes under external illumination taken just prior to each of the ECL photographs. From the resolution of the CCD camera and the characteristics of its lens, one can calculate that each pixel corresponds to approximately a 100 \mu m by 100 \mu m square on the electrode surface. The dark patch seen in the ECL photograph of the $\text{Ru}(\text{dp-bpy})_3^{2+}$ monolayer was due to the air bubble which was trapped during the horizontal transfer and is also seen in the photograph of the electrode under external illumination.

The ECL photographs in Figure 1 give a direct measurement of the distribution of the luminescent Ru complex on the electrode surface. For these ECL photographs to be useful for the characterization of the monolayer on the *air/subphase* interface, the HT transfer must not introduce macroscopic distortions in the monolayer structure. Careful control of the HT transfer conditions is required to achieve this result and has been addressed at length previously.⁷ Of primary importance is that the surface of the electrode be uniformly hydrophobic, oriented closely parallel with the subphase, and brought into contact with the subphase rapidly. For both ECL images shown in Figure 1, the emission of light appears uniform across the surface of the electrode, which is the expected result for a monolayer compressed to its limiting coverage. Within the range of $180\text{--}100 \text{ \AA}^2/\text{molecule}$ the intensity of the ECL was observed to vary linearly with the surface coverage. The uniformity in the ECL emission suggests that the HT transfer has not resulted in collapse or significant distortion of the monolayer film and that the quenching of the amphiphile is uniform across the surface of the electrode. Under these conditions the distribution of the ECL emission from the transferred Ru monolayer should give a good picture of the amphiphile's distribution on the *air/subphase* interface. After the monolayer was aspirated from the Langmuir trough, the removal of the electrode from the subphase and reimmersion caused only minor changes in the ECL pattern for HOPG electrodes and had no effect on the monolayer pattern on ITO electrodes. When the electrode was stepped to 1.2 V (vs Ag/AgCl), both the voltammetric signal and the ECL intensity decreased with time. For 5-min exposures, the ECL intensity decreased by 20–30% for each successive ECL photograph.

The ECL intensity from the $\text{Ru}(\text{bpy})_2(\text{bpy-C}_{19})^{2+}$ monolayer was approximately 2 orders of magnitude more intense than that for the $\text{Ru}(\text{dp-bpy})_3^{2+}$ monolayer. This large difference in the ECL intensity between these two Ru complexes is probably due primarily to more efficient quenching of the electronically excited $\text{Ru}(\text{dp-bpy})_3^{2+}$ by the electrode surface. The difference in the quenching rate of the two complexes may be a function of the hydrocarbon tail present in the $\text{Ru}(\text{bpy})_2(\text{bpy-C}_{19})^{2+}$ which may serve to insulate the headgroup from the electrode surface. Note that the $\text{Ru}(\text{bpy})_2(\text{bpy-C}_{19})^{2+}$ complex orients on the trough with its headgroup on the water and the C_{19} tail toward the air. The HT transfer thus separates the Ru(II) headgroup from the electrode surface by the C_{19} tail.⁶ The Ru(II) center in the $\text{Ru}(\text{dp-bpy})_3^{2+}$ molecule lies closer to the electrode surface. Note that the photoluminescence efficiency of $\text{Ru}(\text{dp-bpy})_3^{2+}$ and its ECL in MeCN solution is higher than that of $\text{Ru}(\text{bpy})_3^{2+}$.² The $\text{Ru}(\text{dp-bpy})_3^{2+}$ complex, when deposited in bilayer and multilayer coverages, displays dramatically enhanced ECL emission. This effect is demonstrated in Figure 3, an ECL photograph of a $\text{Ru}(\text{dp-bpy})_3^{2+}$ monolayer which has been compressed rapidly (barrier speed ca. 0.5 cm/s) to a surface coverage of $100 \text{ \AA}^2/\text{molecule}$. This rapid compression causes localized collapse of the monolayer

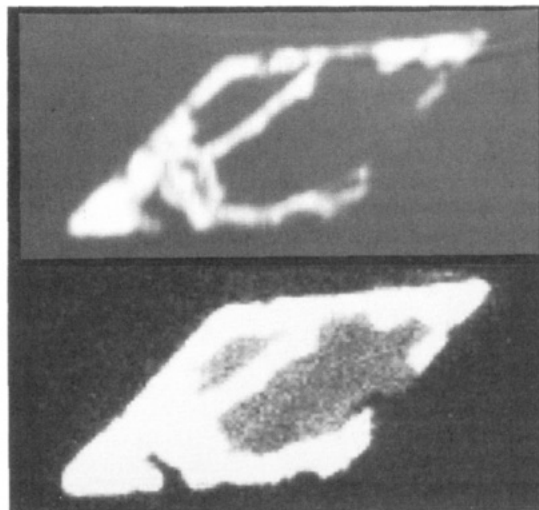


Figure 3. ECL photographs of a partially collapsed monolayer of $\text{Ru}(\text{dp-bpy})_3^{2+}$ at two brightness and contrast settings. The $\text{Ru}(\text{dp-bpy})_3^{2+}$ monolayer was rapidly compressed to ca. $100 \text{ \AA}^2/\text{molecule}$ prior to the horizontal touching (HT) transfer (see text). During the 30-s exposure, the electrode was held at 1.2 V (vs Ag/AgCl).

into multilayer regions on the *air/subphase* interface. Several of these multilayer regions can be seen appearing as bright patches surrounding areas covered with a single monolayer. The ECL intensity from the monolayer patches in Figure 3 is nearly identical to that seen in Figure 1 while the luminescence from the surrounding regions is approximately 2 orders of magnitude more intense. When the average area per molecule of the $\text{Ru}(\text{dp-bpy})_3^{2+}$ on the trough prior to the horizontal transfer and the relative area of the multilayer regions transferred onto the electrode are compared, the bright regions represent, on the average, bilayers of the Ru complex. The ECL intensity from these bright regions is approximately equal to that of the $\text{Ru}(\text{bpy})_2(\text{bpy-C}_{19})^{2+}$ complex.

Comparative Behavior of $\text{Ru}(\text{bpy})_2(\text{bpy-C}_{19})^{2+}$ and $\text{Ru}(\text{dp-bpy})_3^{2+}$ Films. On-trough ECL and electrochemical measurements, in addition to more traditional Π/area determinations, were useful in contrasting the behavior of the two molecules at the *air/water* interface. Although both molecules are insoluble in the aqueous subphase, the C_{19} species is a traditional L-B-type amphiphile with a polar headgroup and a hydrocarbon chain, while the dp-bpy complex contains the Ru(II) center inside a roughly spherical hydrophobic shell, with charge compensating anions in the aqueous phase.

The structural differences between these two ECL-active complexes are also responsible for very different monolayer characteristics on the *air/water* interface. For the Π/area isotherms for these two Ru complexes (Figure 4), at molecular areas above ca. $200 \text{ \AA}^2/\text{molecule}$, the surface pressure is below measurable levels for both Ru complexes. As seen in Figure 4A, compression of the $\text{Ru}(\text{bpy})_2(\text{bpy-C}_{19})^{2+}$ monolayer to $160 \text{ \AA}^2/\text{molecule}$ results in a gradual increase in the surface pressure to 0.1 mN/m . Further compression of the monolayer below $160 \text{ \AA}^2/\text{molecule}$ results in a smooth increase in the surface pressure until the collapse of the monolayer at surface pressures greater than ca. 40 mN/m . Monolayers compressed to 30 mN/m could be reexpanded with little hysteresis in the Π/area isotherm. While the Π/area isotherm of the $\text{Ru}(\text{dp-bpy})_3^{2+}$ (Figure 4B) appears quite similar in shape to that for the $\text{Ru}(\text{bpy})_2(\text{bpy-C}_{19})^{2+}$ complex, several distinct differences are apparent. The surface pressure rises to a measurable level at $170 \text{ \AA}^2/\text{molecule}$ and rises gradually until the monolayer collapses at pressures above 50 mN/m . Reexpan-

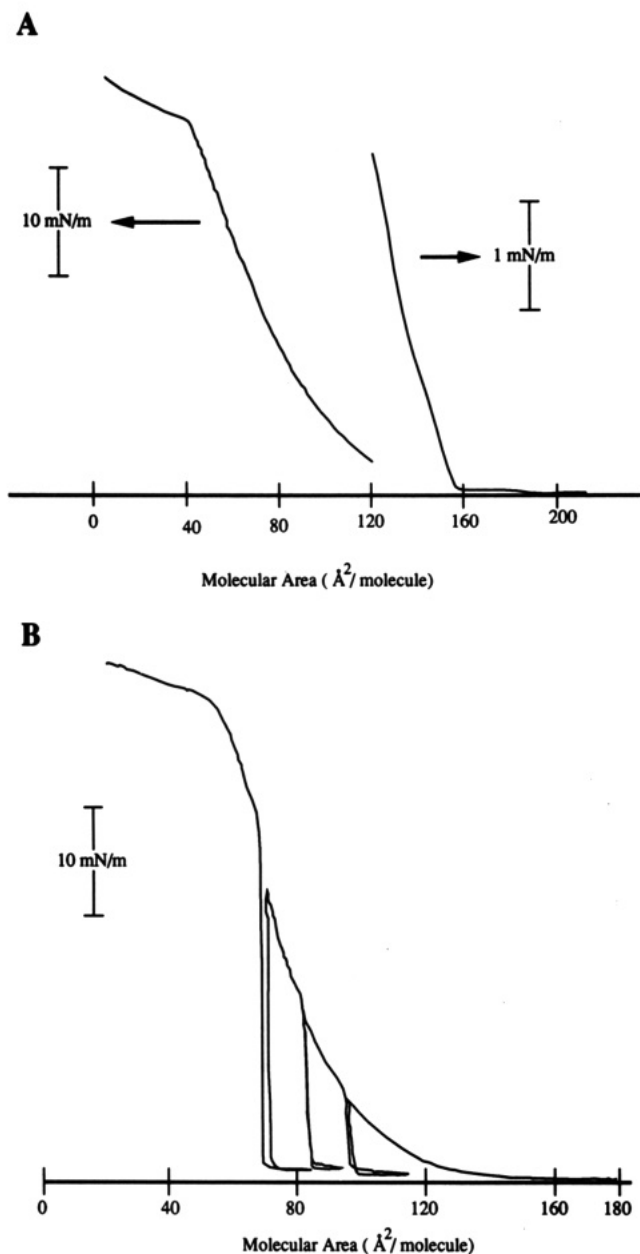


Figure 4. Surface pressure/area isotherms for monolayers of (A) $\text{Ru}(\text{bpy})_2(\text{bpy}-\text{C}_{19})^{2+}$ and (B) $\text{Ru}(\text{dp-bpy})_3^{2+}$. Subphases: (A) 0.3 M Na_2SO_4 , 1.0 mM NaClO_4 ; (B) 0.1 M NaClO_4 . Two surface pressure scales are shown in (A) corresponding to the two segments of the isotherm as indicated. The Π /area isotherm in (B) shows three compression to expansion reversals and the large hysteresis in this isotherm (see text).

sion of the $\text{Ru}(\text{dp-bpy})_3^{2+}$ monolayer at pressures below its collapse point resulted in a rapid decrease in the surface pressure to near zero levels. Upon recompression of the monolayer, the surface pressure remained near zero until the area per molecule decreased below the previous compression, at which point the pressure rapidly increased to follow the previous Π /area curve. Three such compression/expansion reversals are shown in the Π /area isotherm for the $\text{Ru}(\text{dp-bpy})_3^{2+}$ monolayer. The Π /area characteristics of other structurally similar tris(diphenylphenanthroline) complexes, $\text{Ru}(\text{dpp})_3^{2+}$, $\text{Fe}(\text{dpp})_3^{2+}$, and $\text{Co}(\text{dpp})_3^{2+}$, were essentially identical to that of $\text{Ru}(\text{dp-bpy})_3^{2+}$. It is surprising that these symmetrical complexes can form monolayers which withstand extreme surface pressures without collapsing.¹⁶ At first glance,

(16) Watanabe, I.; Hong, K.; Rubner, M. F. *J. Chem. Soc., Chem. Commun.* 1989, 123.

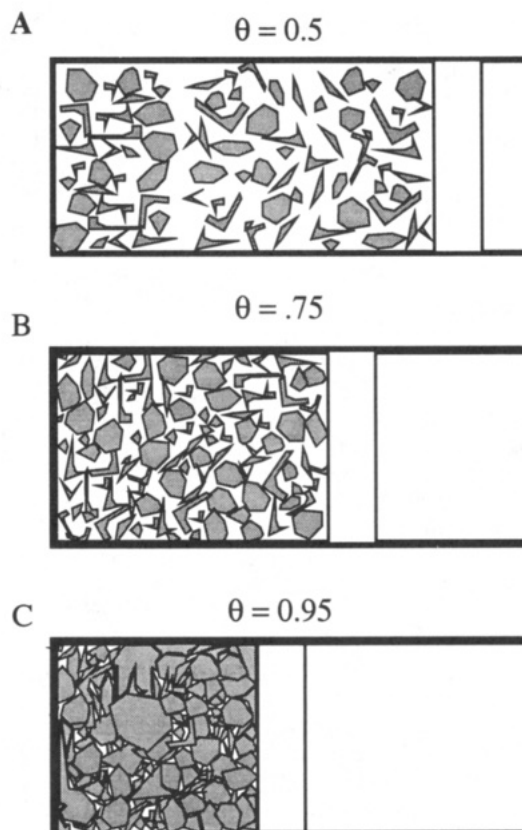


Figure 5. A schematic representation of the aggregation of the diphenylphenanthroline and diphenylbipyridine complexes and the effect of their compression on a Langmuir trough. This shows top views of the trough as the moving barrier compresses the tris complex monolayer to (A) 0.5, (B) 0.75, and (C) 0.95 of the close-packed molecular area.

these tris complexes appear to lack the traditional structure of an amphiphile (i.e., a hydrophobic tail and hydrophilic headgroup). However, because these complexes are charged, one can view the complex as a hydrophobic ball with the counterions as the hydrophilic headgroup. The dramatic hysteresis in the compression and expansion of these monolayers seen in Figure 4 can be explained by assuming the $\text{Ru}(\text{dp-bpy})_3^{2+}$ aggregates into rigid monolayer "rafts" which are compacted rather than compressed as indicated in the schematic representation shown in Figure 5. Figure 5a shows a schematic representation of a $\text{Ru}(\text{dp-bpy})_3^{2+}$ monolayer after its deposition from a HCCl_3 solution on the Langmuir trough. The surface pressure remains zero during the initial compression of the monolayer until, as shown in Figure 5b, the aggregates begin to touch. The rising surface pressure observed upon further compression results from the force required to rotate, fracture, and pack these aggregates so that they conform to the decreasing air/subphase area. Reexpansion of the monolayer causes the surface pressure to drop to zero because these incompressible aggregates do not expand to fill the increasing surface area.

The limiting areas for the $\text{Ru}(\text{bpy})_2(\text{bpy}-\text{C}_{19})^{2+}$ and the tris complexes are governed by the size and packing characteristics of the cationic headgroups. The limiting area for the $\text{Ru}(\text{bpy})_2(\text{bpy}-\text{C}_{19})^{2+}$ complex ($105 \text{ \AA}^2/\text{molecule}$) is in very good agreement with that predicted on the basis of space-filling models, assuming free rotation of the Ru complex ($100 \text{ \AA}^2/\text{molecule}$). The same assumption of free rotation of the tris complexes leads to a predicted molecular area of ca. $300 \text{ \AA}^2/\text{molecule}$. While the incompressibility of the tris complexes and the subsequent large hysteresis in the Π /area isotherms make it difficult to measure the limiting coverage precisely, a

value of ca. $100 \text{ \AA}^2/\text{molecule}$ seems a reasonable estimate. The discrepancy between the observed and predicted molecular areas for the tris complexes strongly suggests significant interpenetration of the pendant phenyl groups. The possible stacking of the phenyl groups between adjacent molecules should increase the tendency of these tris complexes to aggregate into two-dimensional crystallites and severely limit any rotation about the central metal atom. In contrast to molecules of $\text{Ru}(\text{bpy})_2(\text{bpy}-\text{C}_{19})^{2+}$, which has a flexible hydrocarbon chain, the tris complexes have few structural degrees of freedom and so should have a lower entropic barrier to forming crystallites.

Several other experimental results support the presence of these rigid single monolayer aggregates. For the Ru and Fe complexes, these monolayer patches are visible to the naked eye when viewed at normal incidence above a dark background. Due to the large extinction coefficients for these complexes at visible wavelengths, the reflectivity of the air/subphase interface is changed noticeably due to the presence of a single monolayer of these amphiphiles.^{17,18} After a monolayer film was spread from a 0.5 mM solution in HCCl_3 to yield a monolayer with a molecular area of $300 \text{ \AA}^2/\text{molecule}$, irregular light and dark patches with sizes ranging up to ca. 5 mm in diameter were seen at the air/water interface. As the monolayer was compressed, the dark patches decreased in size until at ca. $110 \text{ \AA}^2/\text{molecule}$ when the dark patches disappeared. The presence of the highly adsorbing monolayer increases the reflectivity of the air/subphase interface, resulting in the faintly visible light areas. Monolayer patches of $\text{Fe}(\text{dpp})_3^{2+}$ on the subphase were most easily seen due to its absorbance maximum being at a longer wavelength than that for the Ru complexes. The visible molar absorbances ($\text{M}^{-1} \text{ cm}^{-1}$) in HCCl_3 for $\text{Fe}(\text{dpp})_3^{2+}$, $\text{Ru}(\text{dp-bpy})_3^{2+}$, $\text{Ru}(\text{dpp})_3^{2+}$, and $\text{Bu}(\text{bpy})_2(\text{bpy}-\text{C}_{19})^{2+}$ are $\lambda_{\text{max}} = 536 \text{ nm}$, $\epsilon = 2.3 \times 10^4$; $\lambda_{\text{max}} = 476 \text{ nm}$, $\epsilon = 2.5 \times 10^4$; $\lambda_{\text{max}} = 466 \text{ nm}$, $\epsilon = 3.9 \times 10^4$; $\lambda_{\text{max}} = 458 \text{ nm}$, $\epsilon = 1.5 \times 10^4$, respectively. No variation in the reflectivity of the subphase surface was visible for either the $\text{Co}(\text{dpp})_3^{2+}$ or $\text{Ru}(\text{bpy})_2(\text{bpy}-\text{C}_{19})^{2+}$ complex.

The distribution of the amphiphile between the light and dark patches was assessed by cyclic voltammetry. Upon reexpansion of the monolayer from pressures between 5 and 40 mN/m, the monolayer breaks into much larger aggregates several centimeters squared in area. For this reexpanded film, horizontal transfers were performed over the light and dark regions of the monolayer film. The amount of the amphiphile transferred was assessed by integrating the voltammetric signal for the surface-bound redox-active Ru or Fe complex. Figure 6 shows a typical result of this analysis for the $\text{Fe}(\text{dpp})_3^{2+}$ complex. The amount of the Fe complex transferred in the HT transfer of a light patch is approximately identical to that transferred when the monolayer is held at a constant surface pressure of 15 mN/m. In contrast, the voltammetric signal is nearly zero for transfers of the dark patches. This variability in the voltammetric signal of HT transfers from an expanded monolayer film is very similar to previous voltammetric measurements of highly expanded monolayers of $\text{Ru}(\text{bpy})_2(\text{bpy}-\text{C}_{19})^{2+}$.⁶ An important difference between the variability seen here and that observed previously is that, in this experiment, the level of the voltammetric signal is perfectly predictable because the location of the monolayer aggregates can be seen directly.

The difference in the reflectivity of a single monolayer of these complexes was not sufficiently large to allow the

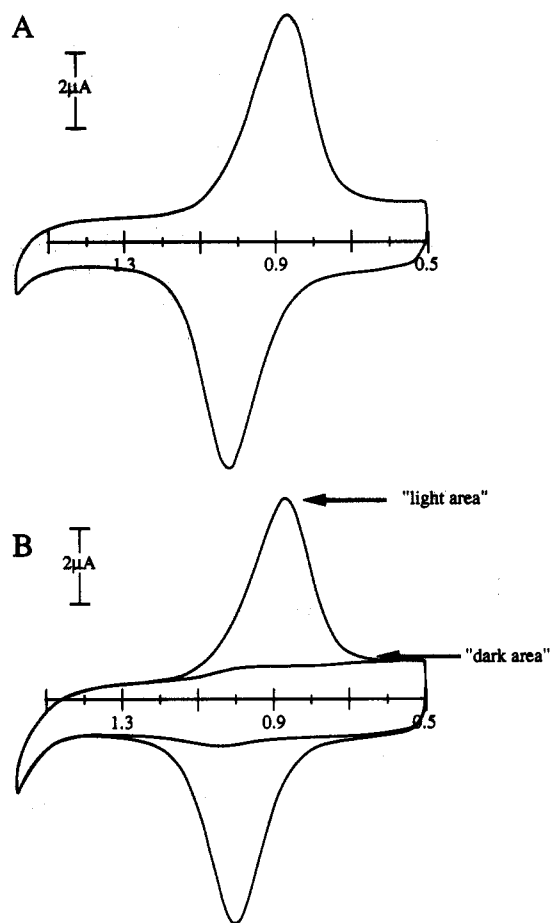


Figure 6. Cyclic voltammograms of transferred monolayers of $\text{Fe}(\text{dpp})_3^{2+}$: (A) obtained using an ITO electrode coated via an HT transfer of a $\text{Fe}(\text{dpp})_3^{2+}$ monolayer held at 15 mN/m; (B) obtained with the same ITO electrode coated via an HT transfer of a "light" and "dark" area of a reexpanded $\text{Fe}(\text{dpp})_3^{2+}$ monolayer (see text).

film to be easily observed from photographs of the air/water interface. However, ECL photographs of a transferred monolayer show quite well these monolayer aggregates. Figure 7 is a photograph of the ECL of a monolayer of $\text{Ru}(\text{dp-bpy})_3^{2+}$ transferred to an ITO electrode. Prior to the HT transfer, the monolayer film was compressed to 30 mN/m and then expanded to a molecular area of $300 \text{ \AA}^2/\text{molecule}$. The monolayer appears as a group of angular patches with a number of fissures induced primarily by the expansion of the monolayer prior to its transfer. The ECL emission appears uniform across each monolayer patch and is approximately equally intense as the monolayer transferred at $120 \text{ \AA}^2/\text{molecule}$ shown in Figure 1. This suggests that the compaction of the monolayer aggregates does not result in multilayer formation which would give rise to a much enhanced ECL intensity.

Formation of Aggregates. A question of interest with film-forming materials at the air/water interface is the extent of molecular aggregation, when the surface pressure is very low. Although this realm of II is usually considered as a two-dimensional gaseous state, nonideal gas behavior could occur in the presence of sufficiently strong intermolecular attraction. In a previous paper from this laboratory⁶ we studied this by HT electrochemical techniques. This can also be studied by on-trough ECL.

The level of aggregation of these monolayers is a strong function of the spreading conditions. When deposited on a clean subphase surface, a HCCl_3 droplet expands at a certain rate, growing the several centimeters in diameter before evaporating. Addition of $\text{Ru}(\text{dp-bpy})_3^{2+}$ to the

(17) Marple, D. T. F.; Vanderslice, T. A. *J. Phys. Chem.* 1960, 64, 1231.

(18) Tweet, A. G. *Rev. Sci. Instrum.* 1963, 34, 1412.

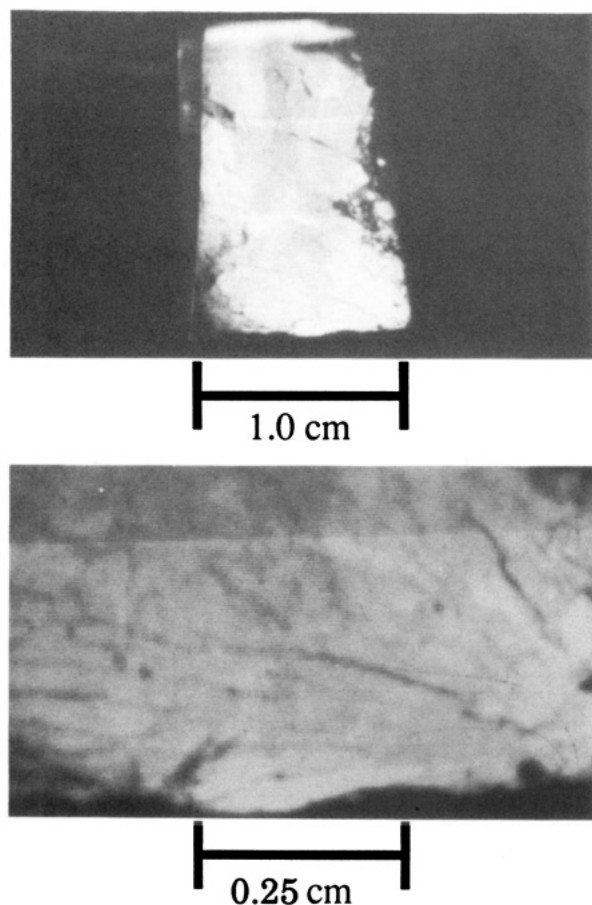


Figure 7. ECL photographs of a Fe(dpp)_3^{2+} monolayer on an ITO electrode at two magnifications. The monolayer was compressed to 15 mN/m and then expanded to $300 \text{ \AA}^2/\text{molecule}$ and the HT transfer made over a mostly "light" area (5-min exposure; electrode width, 1.05 cm).

spreading solvent has no effect on the rate of spreading of the HCCl_3 on the subphase. If the quantity of the complex exceeded a monolayer coverage within the area defined by the expanding HCCl_3 droplet just prior to its complete evaporation, then multilayer aggregates would be formed. Experimentally, we observed that the Π/area isotherms of these tris complexes shifted to lower molecular areas with increasing concentration of the complexes in the spreading solution, consistent with a loss of material from the monolayer film due to the formation of these multilayer aggregates. This can be contrasted with the large increase in the spreading of HCCl_3 droplets containing $\text{Ru(bpy)}_2(\text{bpy-C}_{19})^{2+}$. No change in the Π/area isotherms of this complex was observed with concentration in the spreading solution, even when it was 5 mM . The multilayer aggregates of the tris complexes could be detected visually as small white flakes at the air/subphase interface and were observed whenever the concentration of the complex significantly exceeded 0.5 mM . A $2\text{-}\mu\text{L}$ droplet of a 0.5 mM solution of one of these tris(diphenylphenanthroline) or tris(diphenylbipyridine) complexes would yield a complete monolayer at its limiting molecular area in a circular area 3 cm in diameter. This is approximately the extent of the spreading of the chloroform before its evaporation. More concentrated spreading solutions of these complexes could be used if a small quantity of another surfactant (e.g., arachidic or oleic acid) with a higher equilibrium spreading pressure was mixed in the Ru(dp-bpy)_3^{2+} solution. The second amphiphile increased the rate of spreading of the HCCl_3 droplet; thus, each droplet covered a larger area on the air/subphase interface before its evaporation.

When the concentration of the complex is held well below the 0.5 mM concentration, the amphiphiles should be distributed uniformly within the expanding HCCl_3 layer droplet just prior to its complete evaporation. Through some process of surface diffusion, nucleation, and growth, larger monolayer aggregates form. Indeed, the formation of aggregates on the air/subphase interface was observed to be a requirement for the formation of stable monolayer films of these tris complexes. If the concentration of one of these tris complexes in the spreading solution was lowered below $10 \mu\text{M}$, dissolution of the complex into the subphase competed effectively with this aggregation, resulting in a loss of the complex from the air/subphase interface.⁷ However, once aggregated, no further loss of material from the monolayer was noted.

We were interested in probing the level of aggregation of these monolayer films under highly expanded conditions using ECL photography. A difficulty in addressing the level of aggregation and nonuniformity of Ru(dp-bpy)_3^{2+} and $\text{Ru(bpy)}_2(\text{bpy-C}_{19})^{2+}$ monolayers prior to their compression into compact monolayer films is that the process of depositing the amphiphile on the trough can lead to artifacts in the amphiphile distribution on the air/subphase interface. The expansion of each droplet of the spreading solvent will tend to push amphiphiles at the perimeter of the expanding solvent droplet, producing localized compression. This local compression would be expected to produce aggregates in the same way that large monolayer aggregates are formed upon mechanical compression of the monolayers to ca. $100 \text{ \AA}^2/\text{molecule}$ using the moving barrier of the Langmuir trough. This is a likely cause for the large (up to 5-mm diameter) aggregates observed visually when a monolayer was spread from a 0.5 mM solution of Fe(dpp)_3^{2+} at a molecular area of $300 \text{ \AA}^2/\text{molecule}$. To minimize the compression of the monolayers resulting from the spreading of the monolayer, the concentration of the complexes in the spreading solution was limited to between 0.1 and 0.2 mM , and each droplet was deposited on a different region of the trough surface. The final coverage of the amphiphiles on the Langmuir trough was limited to a small fraction of their limiting coverages. Under these conditions, no variation in the reflectivity of the subphase surface could be detected visually. ECL photography, however, shows clearly that these amphiphiles are not uniformly spread on the air/subphase interface but are localized into a collection of small aggregates. Figure 8 shows ECL photographs of highly expanded monolayers of Ru(dp-bpy)_3^{2+} and $\text{Ru(bpy)}_2(\text{bpy-C}_{19})^{2+}$ obtained at a molecular area of $1000 \text{ \AA}^2/\text{molecule}$. For the expanded monolayers of Ru(dp-bpy)_3^{2+} (Figure 8A), several light patches ranging from ca. 0.4 to 1.0 mm in diameter are seen on the electrodes.

The transfers of monolayers of $\text{Ru(bpy)}_2(\text{bpy-C}_{19})^{2+}$ at $1000 \text{ \AA}^2/\text{molecule}$ (Figure 8B) also show a nonuniform distribution on the electrode surface. The localized areas of ECL emission are similar in size to those of the Ru(dp-bpy)_3^{2+} monolayer but have a more diffuse perimeter. It is apparent that some of the $\text{Ru(bpy)}_2(\text{bpy-C}_{19})^{2+}$ is present at a lower density over a larger region of the electrode. From a comparison of the intensity of the ECL emissions between these aggregates and a full monolayer coverage shown in Figure 1, one can estimate that the aggregates formed are roughly equivalent in coverage to a monolayer with a molecular area of ca. $120 \text{ \AA}^2/\text{molecule}$ for Ru(dp-bpy)_3^{2+} and ca. $300 \text{ \AA}^2/\text{molecule}$ for $\text{Ru(bpy)}_2(\text{bpy-C}_{19})^{2+}$. The $\text{Ru(bpy)}_2(\text{bpy-C}_{19})^{2+}$ aggregates are much less compact than the Ru(dp-bpy)_3^{2+} . Confirming evidence for this assessment was obtained by taking ECL photographs of monolayers transferred after these highly expanded monolayers were compressed to ca. $300 \text{ \AA}^2/$

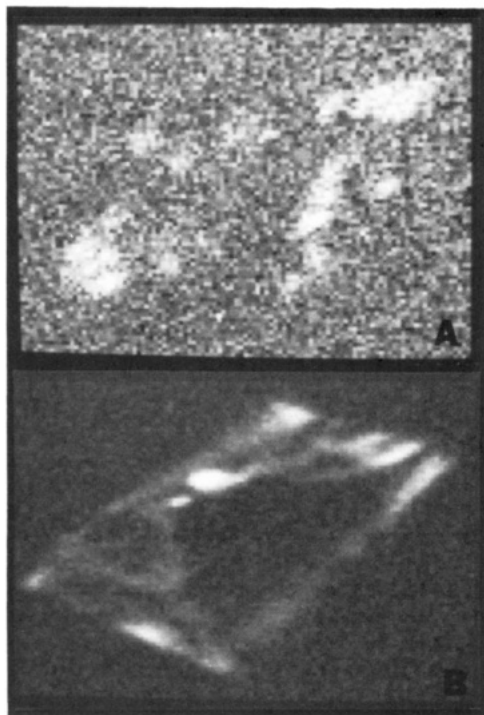


Figure 8. ECL photographs of highly expanded monolayers of (A) $\text{Ru}(\text{dp-bpy})_3^{2+}$ and (B) $\text{Ru}(\text{bpy})_2(\text{bpy-C}_{19})^{2+}$. Monolayers were transferred onto HOPG electrodes at $1000 \text{ \AA}^2/\text{molecule}$ (30-s exposure).

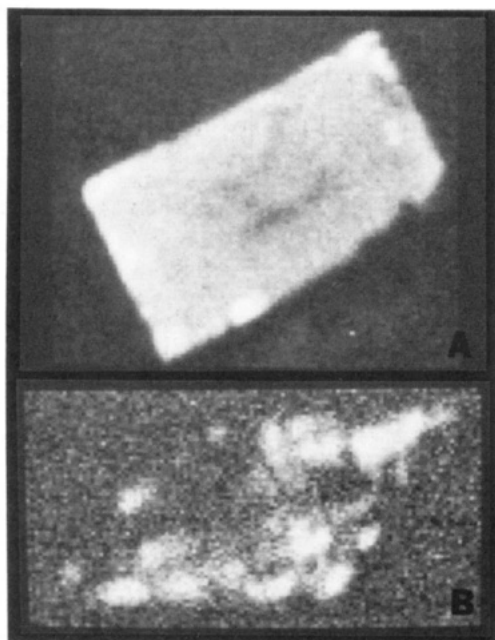


Figure 9. ECL photographs of (A) $\text{Ru}(\text{bpy})_2(\text{bpy-C}_{19})^{2+}$ and (B) $\text{Ru}(\text{dp-bpy})_3^{2+}$ monolayers. Monolayers were initially deposited under the same experimental conditions as those in Figure 8 and then compressed to 290 and $320 \text{ \AA}^2/\text{molecule}$, for (A) and (B), respectively.

molecule. Figure 9 shows ECL photographs of $\text{Ru}(\text{bpy})_2(\text{bpy-C}_{19})^{2+}$ and $\text{Ru}(\text{dp-bpy})_3^{2+}$ monolayers transferred at 290 and $320 \text{ \AA}^2/\text{molecule}$, respectively. The $\text{Ru}(\text{bpy})_2(\text{bpy-C}_{19})^{2+}$ monolayer shown in Figure 9A is quite uniform; this signals the coalescence of the aggregates. The $\text{Ru}(\text{dp-bpy})_3^{2+}$ monolayer, in contrast, is heterogeneous, displaying the same small aggregates seen in Figure 8.

The aggregation seen in the ECL photographs in Figures 8 and 9 occurs with the amphiphiles under extremely low or zero surface pressure. From the Π/area isotherm of $\text{Ru}(\text{bpy})_2(\text{bpy-C}_{19})^{2+}$ shown in Figure 4A, the highest coverage that would be possible for this amphiphile would be ca. $200 \text{ \AA}^2/\text{molecule}$. This is the molecular area at which the monolayer displays a measurable surface pressure. The estimate of the coverage of the aggregates obtained from ECL photography is therefore in reasonable agreement with that predicted by the isotherm in Figure 4. By compressing the $\text{Ru}(\text{dp-bpy})_3^{2+}$ monolayer to ca. $100 \text{ \AA}^2/\text{molecule}$ and then reexpanding to $110 \text{ \AA}^2/\text{molecule}$, this monolayer can be present at near limiting area coverage and yet have no measurable surface pressure as seen in Figure 4B.

Conclusions

ECL photography is a potentially powerful technique for studying monolayer films. Because of the electrochemical excitation of the luminescent probe, the experimental apparatus is significantly simplified when compared to fluorescence techniques. The light emitted from a monolayer of a luminescent probe such as $\text{Ru}(\text{bpy})_2(\text{bpy-C}_{19})^{2+}$ is several orders of magnitude higher than the detection limit of the CCD camera used in this study. A small fraction of a monolayer could therefore be imaged easily with this technique. The sensitivity of the ECL photography could then allow one to study nonluminescent monolayers by adding a small quantity of an ECL-active amphiphile as a luminescent probe as is done in fluorescence microscopy. As demonstrated by the large difference in the ECL efficiency between $\text{Ru}(\text{bpy})_2(\text{bpy-C}_{19})^{2+}$ and $\text{Ru}(\text{dp-bpy})_3^{2+}$ monolayers, special emphasis must be placed on the structure of potential ECL probes to minimize their quenching by the electrode surface. These results also reinforce our earlier suggestions^{1,5} concerning the use of adsorbed ECL emitting species as an approach to high-sensitivity detection of very small amounts (submonolayers) of these materials.

ECL photographs of $\text{Ru}(\text{bpy})_2(\text{bpy-C}_{19})^{2+}$ and $\text{Ru}(\text{dp-bpy})_3^{2+}$ monolayers transferred to HOPG and ITO electrodes clearly show that aggregation of the amphiphiles occurs at very low or zero surface pressure prior to their compression. The aggregations of the tris(diphenylphenanthroline) and tris(diphenylbipyridine) complexes are also supported by direct visual observations and electrochemical measurements. These symmetrical amphiphiles are a new and interesting class of Langmuir monolayers. Their resistance to collapse and small limiting molecular areas suggest an intimate interaction of their diphenyl moieties. While we have no evidence about what determines the degree of crystallinity of these monolayers, it seems reasonable that the aggregates are in the form of microcrystallites which adhere into the larger aggregates observed in the ECL photographs. The effect of the compaction/compression of these crystallites in the Langmuir balance, the possibility of annealing the monolayer into large single two-dimensional crystals, and their study by X-ray or electron diffraction techniques are questions of current interest.

Acknowledgment. The support of this research by the National Science Foundation (Grant CHE8901450) and the Robert A. Welch Foundation is gratefully acknowledged.